Supplementary Information

An injectable, electroconductive hydrogel/scaffold for neural repair and motion sensing

Junpeng Xu[1], Chui-Wei Wong[1], Shan-hui Hsu[1,2,*]

[1] Institute of Polymer Science and Engineering, National Taiwan University, No. 1, Sec. 4 Roosevelt Road, Taipei 10617, Taiwan, Republic of China

[2] Institute of Cellular and System Medicine, National Health Research Institutes, No. 35 Keyan Road, Miaoli 35053, Taiwan, Republic of China

Pages: 15

Supplemental tables: 2 (Table S1 and Table S2)

Supplemental figures: 11 (Figure S1 – S11)

Supplemental videos: 5 (Movies S1 – S5)

* Corresponding author: Shan-hui Hsu

Institute of Polymer Science and Engineering, National Taiwan University, No. 1, Sec. 4 Roosevelt Road, Taipei 10617, Taiwan, R.O.C.;

Phone: +886-2-3366-5313;

Fax: +886-2-3366-5237;

E-mail: shhsu@ntu.edu.tw

Table S1. The zeta potential and hydrodynamic diameter of CEC, DCP, and DFPU.

Sample	Zeta potential (mV)	Hydrodynamic diameter (nm)
CEC	-41.20 ± 2.44	/
DCP	+20.98 ± 0.78	137.52 ± 19.67
DFPU	-43.18 ± 1.02	36.67 ± 2.47

Table S2. Conductivity of CDD hydrogels (CDDH) and scaffolds (CDDS) comprising different solid contents of DCP nanoparticles.

Sample	DCP (wt%)	CEC (wt%)	DFPU (wt%)	Conductivity ($mS \cdot cm^{-1}$)
CDDH0	0	3	3	0.88 ± 0.11
CDDH5	0.01	3	3	2.54 ± 0.13
CDDH6	0.02	3	3	3.13 ± 0.27
CDDH2	0.03	3	3	5.85 ± 0.33
CDDH7	0.04	3	3	4.62 ± 0.39
CDDH8	0.05	3	3	4.20 ± 0.26
CDDS0	0	3	3	0.53 ± 0.09
CDDS5	0.01	3	3	2.05 ± 0.19
CDDS6	0.02	3	3	2.89 ± 0.15
CDDS2	0.03	3	3	3.83 ± 0.34
CDDS7	0.04	3	3	3.58 ± 0.31
CDDS8	0.05	3	3	3.62 ± 0.27

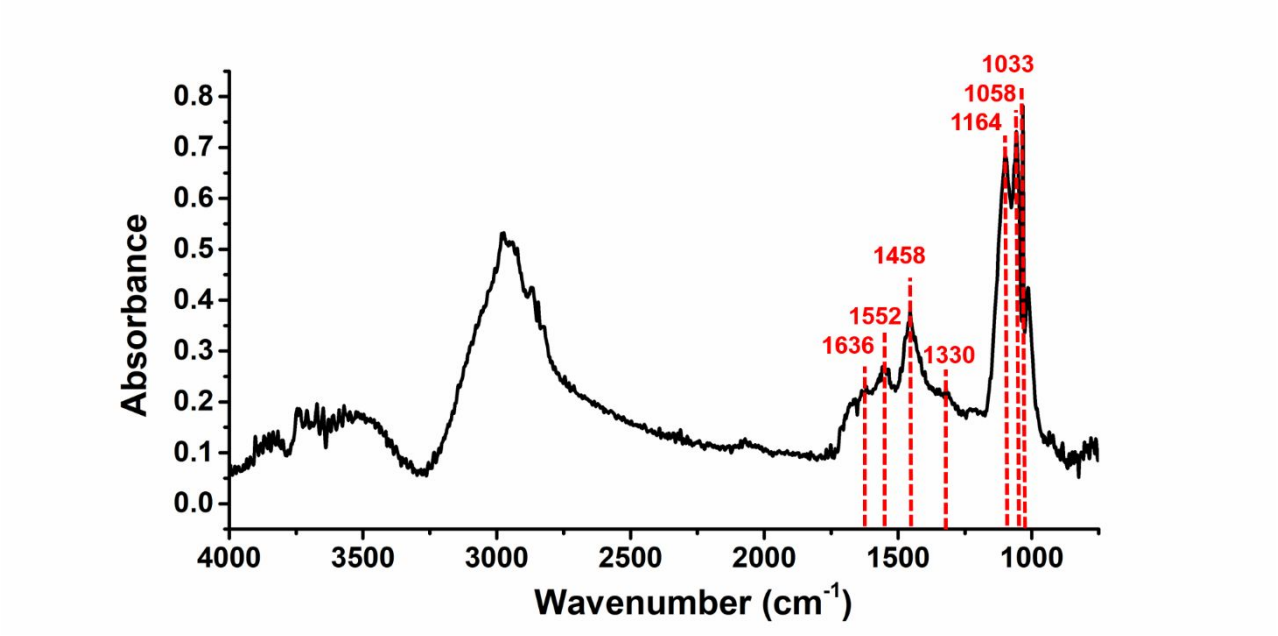

Figure S1. The IR spectrum of DCP.

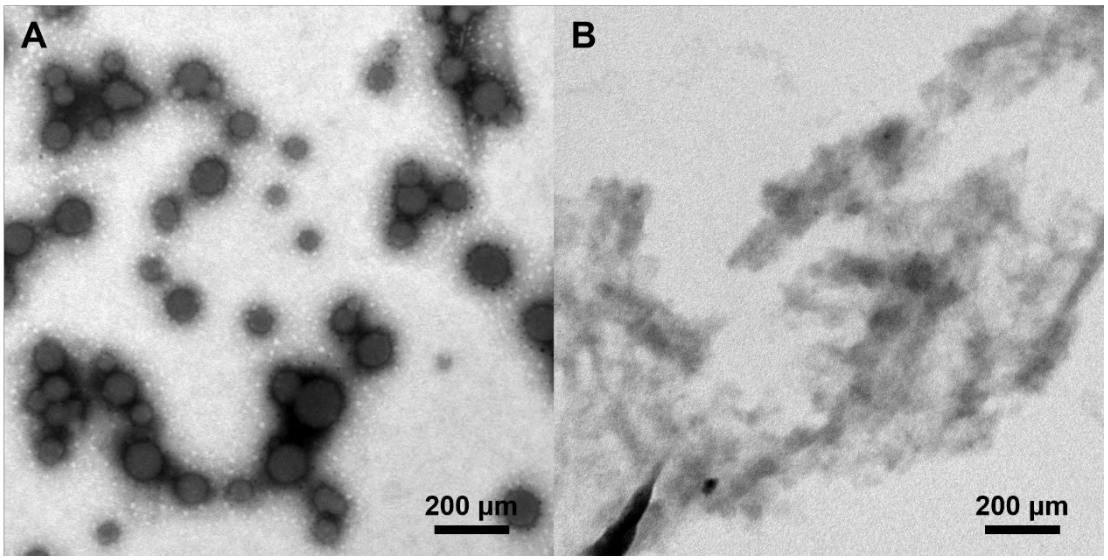

Figure S2. TEM images of (A) DFPU and (B) CEC.

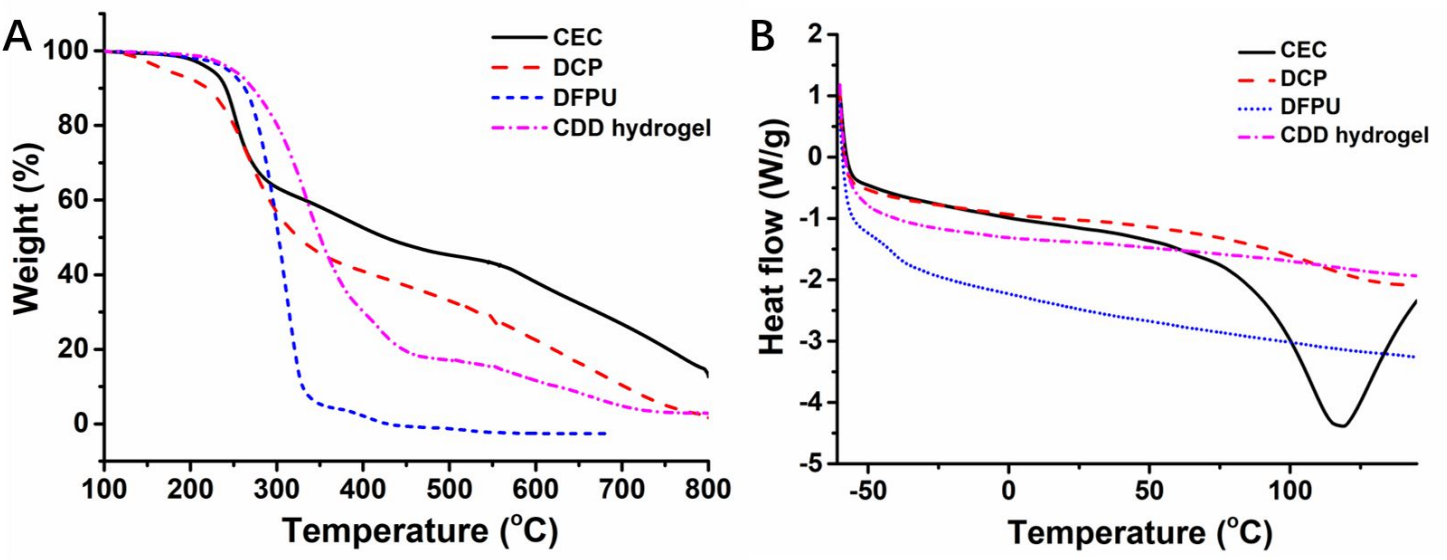

Figure S3. Thermal properties of CDD hydrogels and each component of the materials, by (A) thermogravimetric analysis and (B) differential scanning calorimetry.

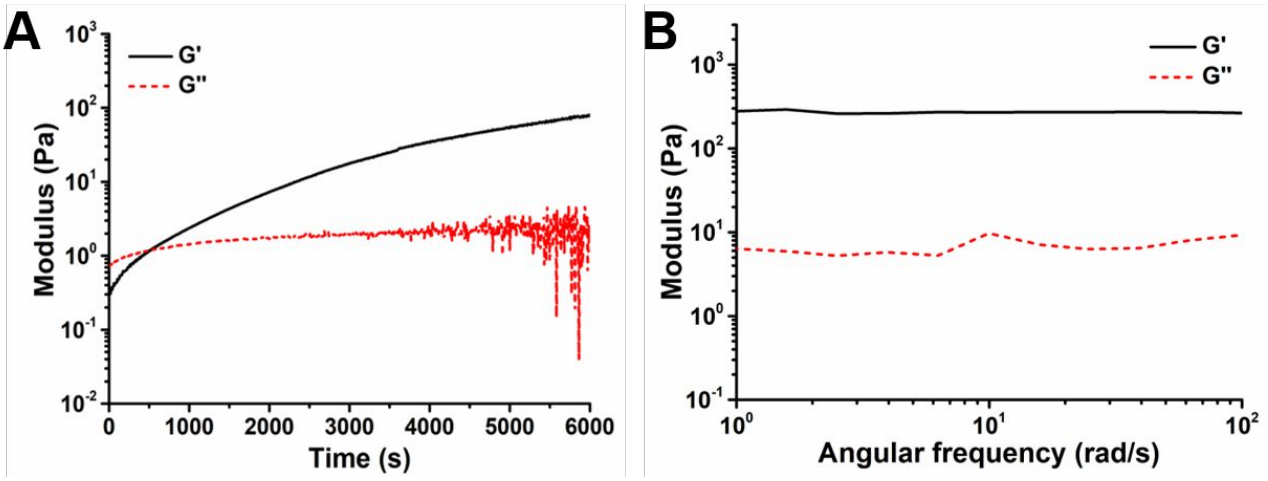

Figure S4. The time-dependent and frequency-dependent viscoelasticity of CDD hydrogels at 37 °C and 1% strain. (A) Samples were loaded after mixing of CDD hydrogel components and measured immediately for time-dependent changes of G' and G''. Gelation occurred at ~480 s. (B) Samples were measured after gelation for frequency-dependent changes of equilibrium G' and G''.

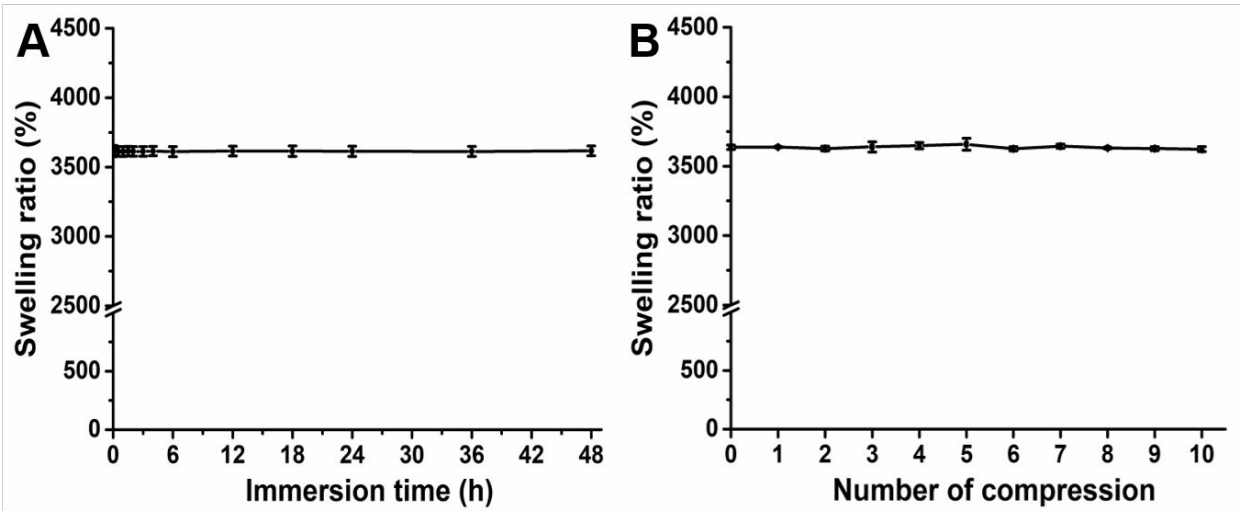

Figure S5. Swelling experiment for CDD scaffolds. (A) Nearly unchanged swelling ratios against the time after immersion of CDD scaffolds in PBS. (B) Nearly unchanged swelling ratios after multiple cycles of compression and recovery.

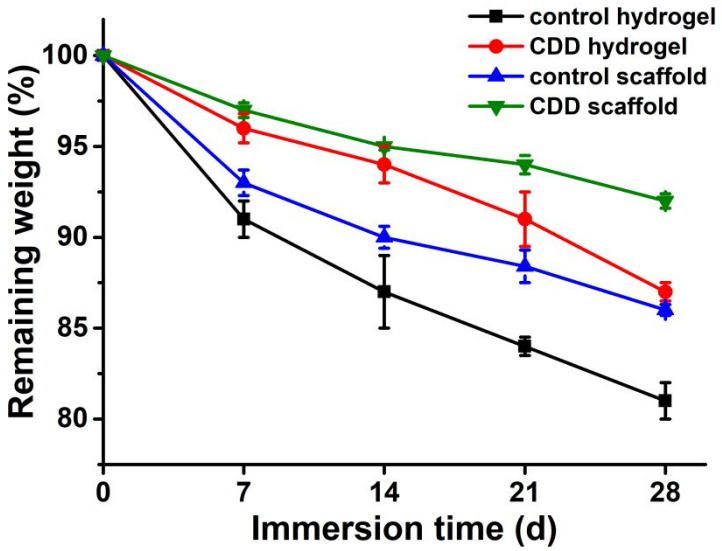

Figure S6. In vitro degradation of CDD hydrogel and scaffolds analyzed at 7, 14, 21, and 28 days in 37 °C PBS. The control hydrogel and control scaffold are the hydrogel and scaffold without DCP. Note that these in vitro results were very different from those in vivo, which is common for chitosan-based materials.

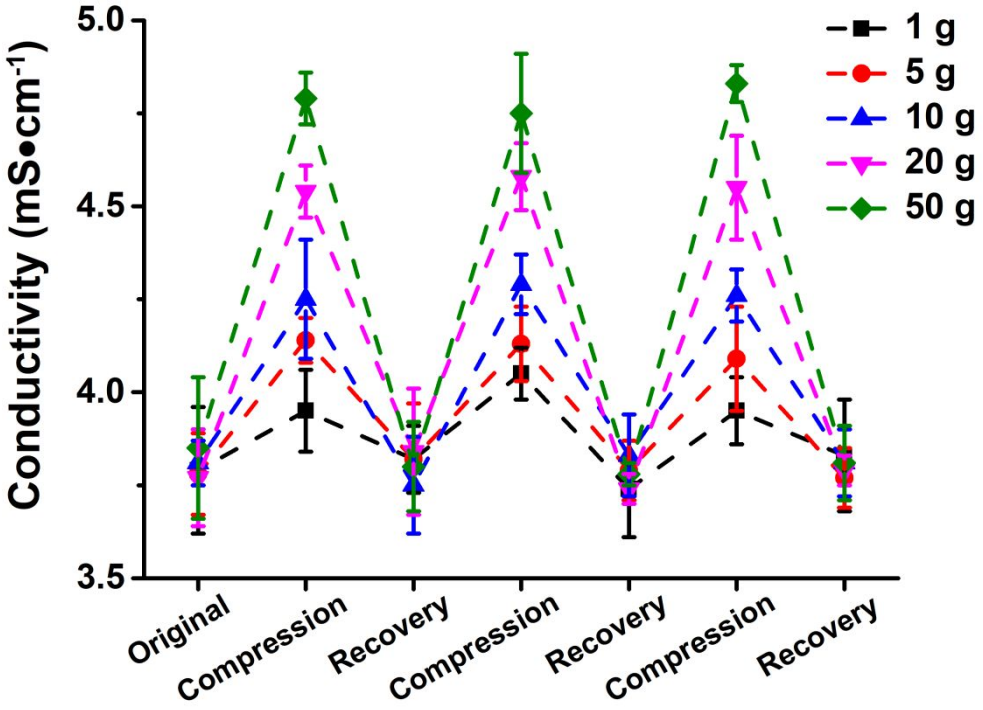

Figure S7. Repeated sensing of the compressive strain for the CDD scaffolds bearing different weights under 0.5 V of applied voltage.

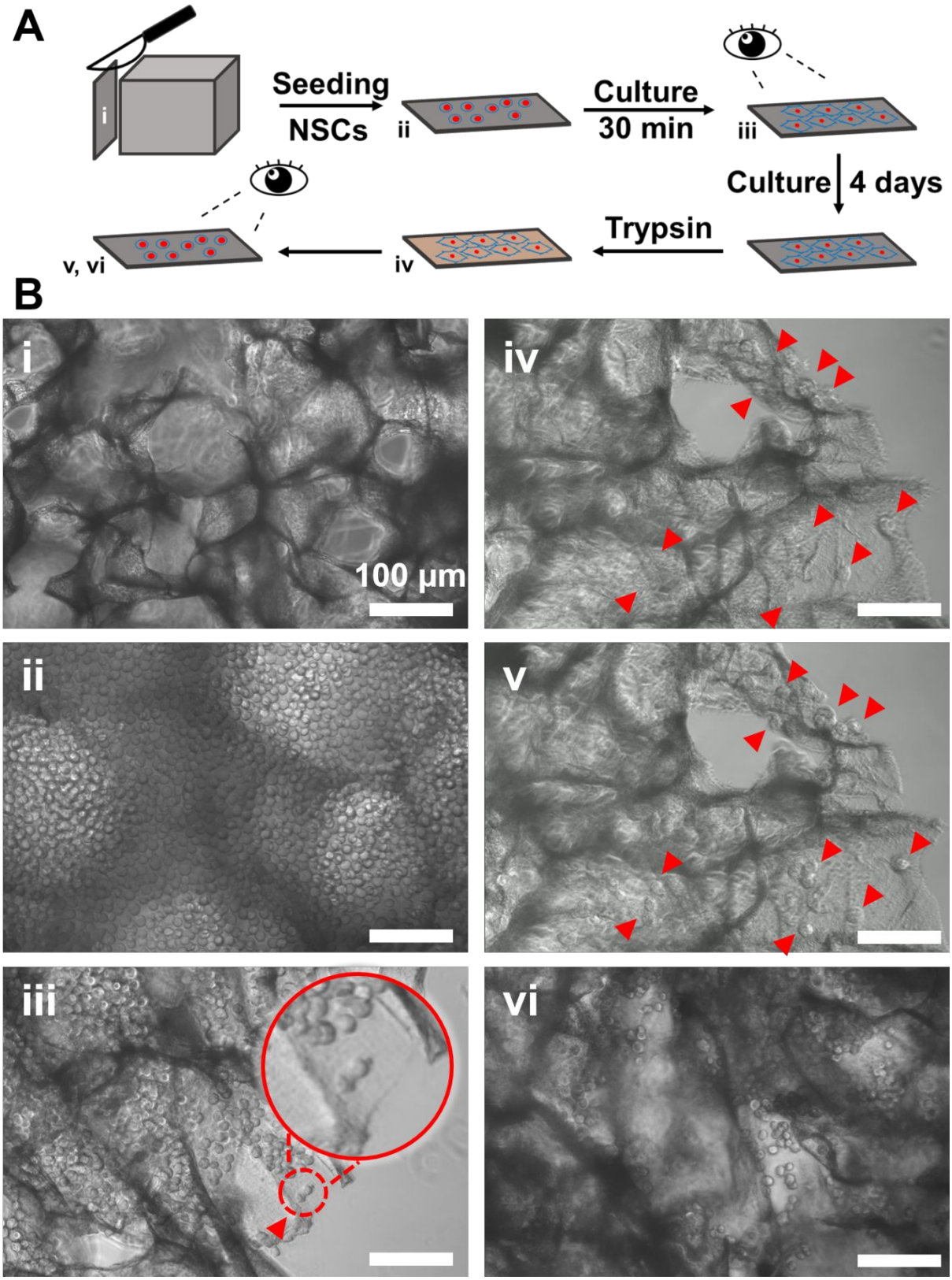

Figure S8. Cell adhesion assay to confirm the attachment of NSCs in CDD scaffolds. (A) A schematic showing the procedures in the cell adhesion

assay. (B) Optical microscopic images of the hydrated CDD scaffold slice: (i) the initial CDD scaffold slice (1 cm × 0.5 cm, ~10 μm in thickness) without cells; (ii) the CDD scaffold slice seeded with 4×10^5 NSCs per slice; (iii) the NSC-seeded CDD scaffold slice after incubation for 30 min; (iv) the NSC-containing CDD scaffold slice cultured for 4 days, followed by observation at once after the addition of trypsin. (v) After the trypsin treatment for 10 min, the NSCs had obvious morphological alteration, indicated by red arrows. (vi) After the trypsin treatment for 30 min, NSCs obviously detached from the CDD scaffold. The enlarged circular area in (iii) indicates the location where cells were attached. A real-time recording video was also provided (Movie S4).

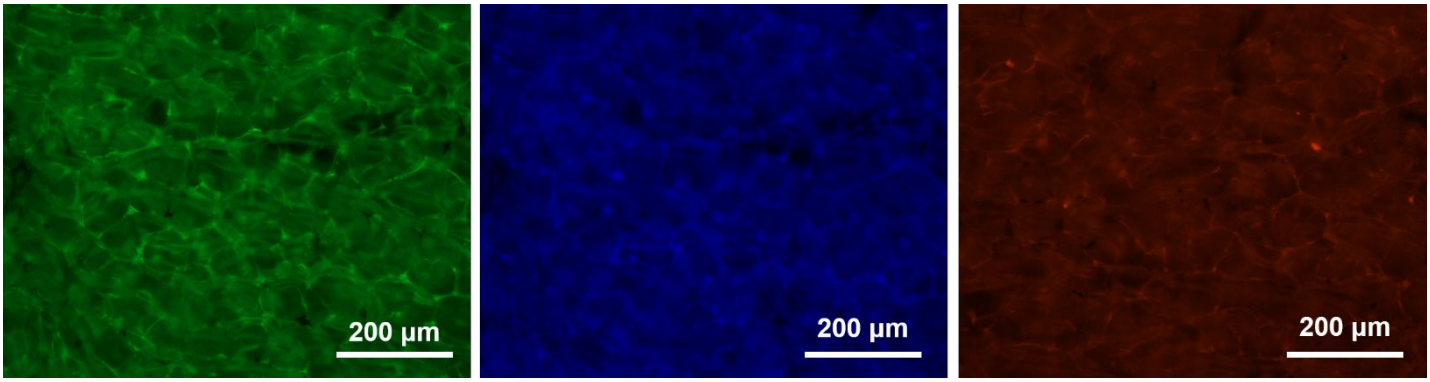

Figure S9. The auto-fluorescence property of the CDD scaffold under the different conditions of fluorescence detection.

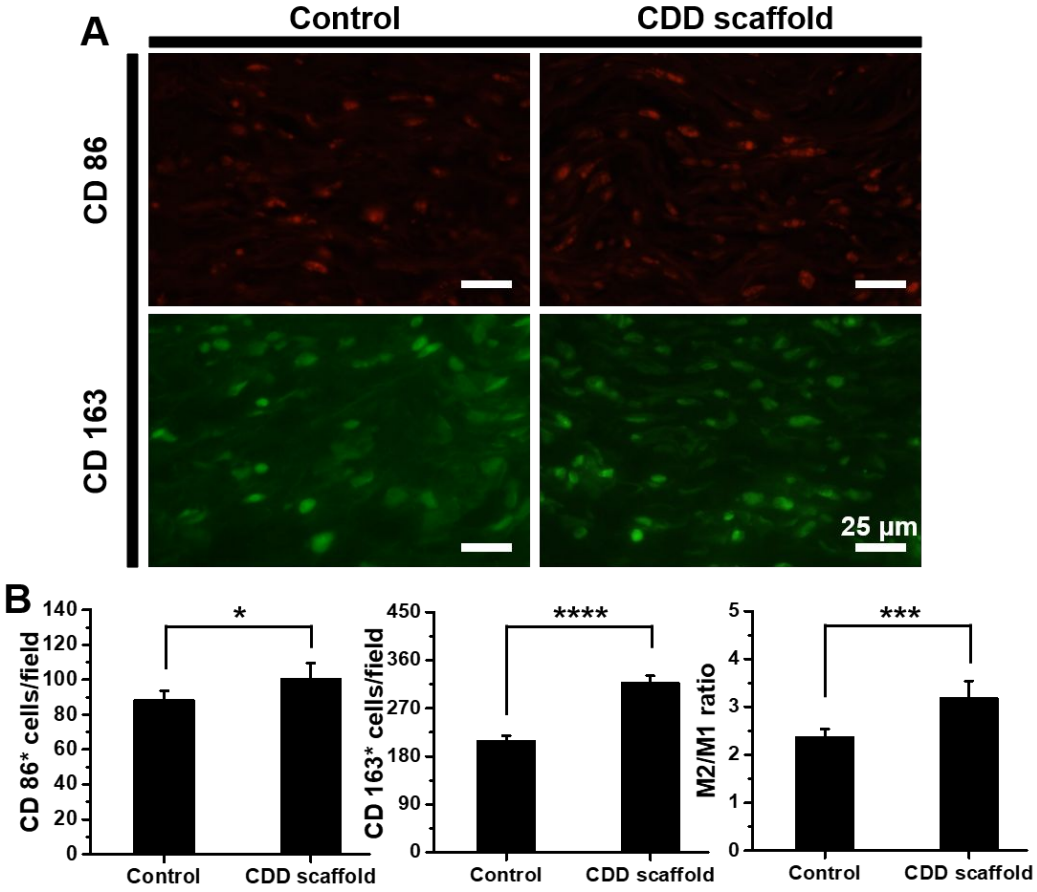

Figure S10. The distribution of M1 and M2 macrophages in the explanted tissue of rats after subcutaneous implantation for 14 days by the marker protein immunofluorescence staining. (A) Immunofluorescent images of CD86 positive M1 macrophages (red) and CD163 positive M2 macrophages (green). (B) Quantification the population of M1 and M2 macrophages and the population ratios of M2/M1. Results are expressed as mean ± SD, N = 3. *$p < 0.05$, ***$p < 0.001$, and ****$p < 0.0001$ among the indicated groups. Control group: scaffolds without DCP.

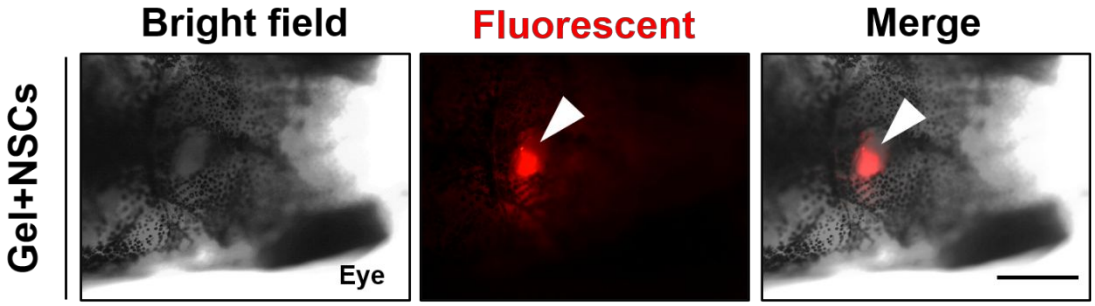

Figure S11. Tracking for the location of the CDD hydrogel (with auto-fluorescence) injected into the adult zebrafish brain under the bright field and red filter. Scale bar indicate 1 mm.

Movie S1. Fast shape recovery. Scaffolds crumpled up can quickly recover their shape after hydration.

Movie S2. Confocal 3D structure. The confocal microscopy reveals the 3D network of CDD scaffolds from different viewing angles.

Movie S3. Injectable scaffolds. Scaffolds with triangle sheet shape (4 mm × 3 mm × 1 mm) injected into a water bath using the 20G needle can retain their original shape.

Movie S4. Cell morphology. The continuous changes in cell morphology of NSCs during the cell detachment from the CDD scaffold.

Movie S5. Motor function recovery. The motor function recovery effect of brain-injured zebrafish treated with PBS, CDD hydrogel, and NSC-laden CDD hydrogel after 6 days.